

Sequential FRET Processes in Calix[4]arene-Linked Orange-Red-Green Perylene Bisimide Dye Zigzag Arrays

Catharina Hippus,[†] Ivo H. M. van Stokkum,[§] Marcel Gsänger,[†] Michiel M. Groeneveld,[‡] René M. Williams,^{*,‡} and Frank Würthner^{*,†}

Institut für Organische Chemie and Röntgen Research Center for Complex Material Systems, Universität Würzburg, Am Hubland, D-97074 Würzburg, Germany, Molecular Photonics Group, van't Hoff Institute for Molecular Sciences (HIMS), Universiteit van Amsterdam, Nieuwe Achtergracht 129, 1018 WV Amsterdam, The Netherlands, and Department of Physics and Astronomy, Vrije Universiteit, de Boelelaan 1081, 1081 HV Amsterdam, The Netherlands

Received: November 22, 2007

Perylene bisimide–calix[4]arene arrays composed of up to three different types of perylene bisimide chromophores (orange, red, and green PBIs) have been synthesized. Within these arrays, the individual chromophoric building blocks are positioned in defined spatial orientation and are easily replaceable by each other without influencing the overall geometric arrangement of the supramolecular system. The specific optical properties of the individual chromophore facilitated the investigation of photoinduced processes very accurately by time-resolved emission and femtosecond transient absorption spectroscopy. A quantitative analysis of the photophysical processes as well as their rate constants have been obtained by employing UV/vis absorption, steady state and time-resolved emission, femtosecond transient absorption spectroscopy, and spectrotemporal analysis of the femtosecond transient absorption data. These studies reveal very efficient energy transfer processes from the orange to the red PBI chromophoric unit ($k_{ET} = 6.4 \times 10^{11} \text{ s}^{-1}$ for array **or**), from the red to the green PBI ($k_{ET} = 4.0 \times 10^{11} \text{ s}^{-1}$ for array **rg**), and slightly less efficient from the orange to the green PBI ($k_{ET} = 1.5 \times 10^{11} \text{ s}^{-1}$ for array **og**) within these perylene bisimide–calix[4]arene arrays. The experimentally obtained rate constants for the energy transfer processes are in very good agreement with those calculated according to the Förster theory.

Introduction

Photosynthesis in plants and bacteria represents one of the most important biological processes responsible for the development and sustenance of life on earth.¹ It has been demonstrated that, for example, in purple bacteria the primary steps of photosynthesis involve the absorption of photons by light-harvesting multichromophoric antenna complexes and subsequent directional transport of the energy through excited-state energy transfer to the photosynthetic reaction centers. The high efficiency of natural photosynthesis is thus an outcome of proper organization of a multitude of chromophores in space that exhibit distinct absorption, emission, and redox properties. Inspired by such biofunctional systems, many organic chemists aim at artificial structures containing multiple chromophores that provide sequential energy transfer, and functional dye assemblies possessing energy and charge transport properties for mimicking the fundamental processes of photosynthesis have thus attracted considerable attention in materials as well as in biological sciences in the past years.^{2,3}

Accordingly, the synthetic approach toward artificial structures based on organized functional dyes aims at the defined spatial arrangement of multiple chromophores to ensure efficient sequential energy transfer processes between the individual dye units.⁴ Numerous classes of functional dyes have been employed

to design multichromophoric architectures, among those perylene bisimides (PBIs) have been shown to be particularly useful for the investigation of light-harvesting energy transfer processes,^{5–7} as PBIs are highly fluorescent with quantum yields up to unity, chemically inert, and exceptionally photostable.⁸ Thus, perylene bisimides (among other classes of functional dyes) have been successfully applied to afford a variety of covalently constructed and self-assembled light-harvesting architectures such as rigid linear arrays of chromophores linked by spacer units,^{5,9} molecular squares^{7a,b,10} as well as dendrimers (in general, with energy transfer from peripheral chromophores to the core dye).^{6,11} The spatial arrangements of the chromophoric units in different dye architectures are schematically shown in Figure 1. Furthermore, numerous examples of π – π -stacked supramolecular dye aggregates^{3,12,13} exist as well. In contrast, only a few examples of covalent stacked arrangements of dyes (Figure 1) are given which are typically limited to bichromophoric systems, as in most cases only dimeric units,^{14,15} or systems of less defined geometry have been realized.¹⁶ This might be due to the following reasons: (i) There are only few well-defined rigid scaffolds available that provide good solubility as required for obtaining longer oligomers and (ii) such architectures require a set of dyes with tunable absorption and emission properties without extension of the molecular lengths or the direction of the transition dipole moment upon variation of the optical properties.

In this context, a new design principle for artificial light-harvesting architectures has been suggested by our group aiming at stacked arrangements of PBI chromophores by positioning

* To whom correspondence should be addressed. E-mail: wuerthner@chemie.uni-wuerzburg.de; williams@science.uva.nl.

[†] Universität Würzburg.

[‡] Universiteit van Amsterdam.

[§] Vrije Universiteit.

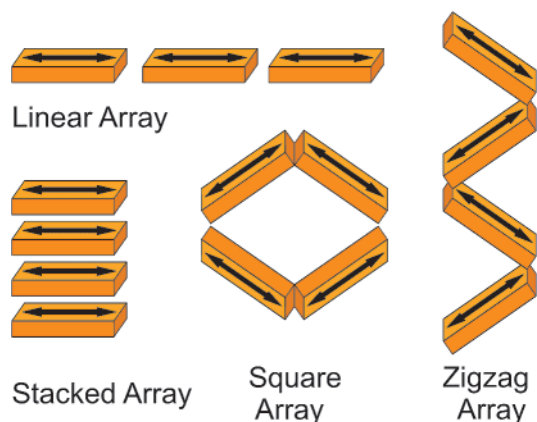


Figure 1. Schematic representation of different types of spatial arrangements of chromophoric units in supramolecular dye architectures.

the dye units with their transition dipole moments orthogonally to a structurally defined repetitive molecular framework (see Figure 1, left). For this purpose, calix[4]arenes¹⁷ seemed to be good candidates that have been previously utilized for the organization of nonlinear optical dyes,¹⁸ electrophores,¹⁹ and fluorophores,²⁰ as well as self-assembled species by, e.g., hydrogen bonding,²¹ or metal-ion coordination.²² However, as we show in this work, the structural organization of PBI dyes along a calix[4]arene-based scaffold is better described by a zigzag chain (Figure 1, right) which still provides a very favorable situation for highly efficient sequential fluorescence energy transfer (FRET).

PBI dyes represent an outstanding class of chromophores for stacked or zigzag architectures with well-defined orientation of the respective transition dipole moments (see arrows in Figure 1), and this versatile chromophore can be easily fine-tuned by proper substituents in the so-called bay positions to exhibit quite diverse electronic and optical properties.⁸ As such, the classes of phenoxy- (red)²³ and pyrrolidino- (green)²⁴ bay-substituted PBIs as well as core-unsubstituted derivatives (orange)⁸ are available; thus a broad section of the visible spectrum can be utilized for light harvesting purposes. In this regard, we and others have recently reported the first examples of orange, red, or green PBI dyes connected to calix[4]arene scaffolds to organize the functional dye units.^{25–28} Recently, we have communicated the construction of calix[4]arene-erylene bisimide arrays based on up to five perylene bisimide units revealing efficient energy transfer processes between the chromophores.²⁷ Here we report our detailed studies of an extensive series of PBI–calix[4]arene arrays and elucidate by means of femtosecond transient absorption spectroscopy whether the efficiency of the energy transfer processes is substantially influenced by the specific positioning and number of the respective energy donor and energy acceptor dye units.

Toward this goal, we have synthesized a broad series of PBI–calix[4]arene arrays (see Scheme 1) that are composed of up to three different types of PBI chromophores, i.e., orange (absorption maxima at 526 and 490 nm), red (absorption maximum at 578 nm), and green (absorption maximum at 701 nm) PBIs which we denote here as **o**, **r**, and **g**, respectively. These PBI chromophores are linked by calix[4]arene spacers (**c**) through the N-imide bond of PBI, and thus three different types of arrays have been realized: The first type is composed of two chromophoric units and they are named as **or**, **rg**, and **og**, respectively, according to the combination of the respective PBI units. The second type of arrays is composed of three different chromophoric PBI units and they are denoted as **oro**, **ror**, **rgr**,

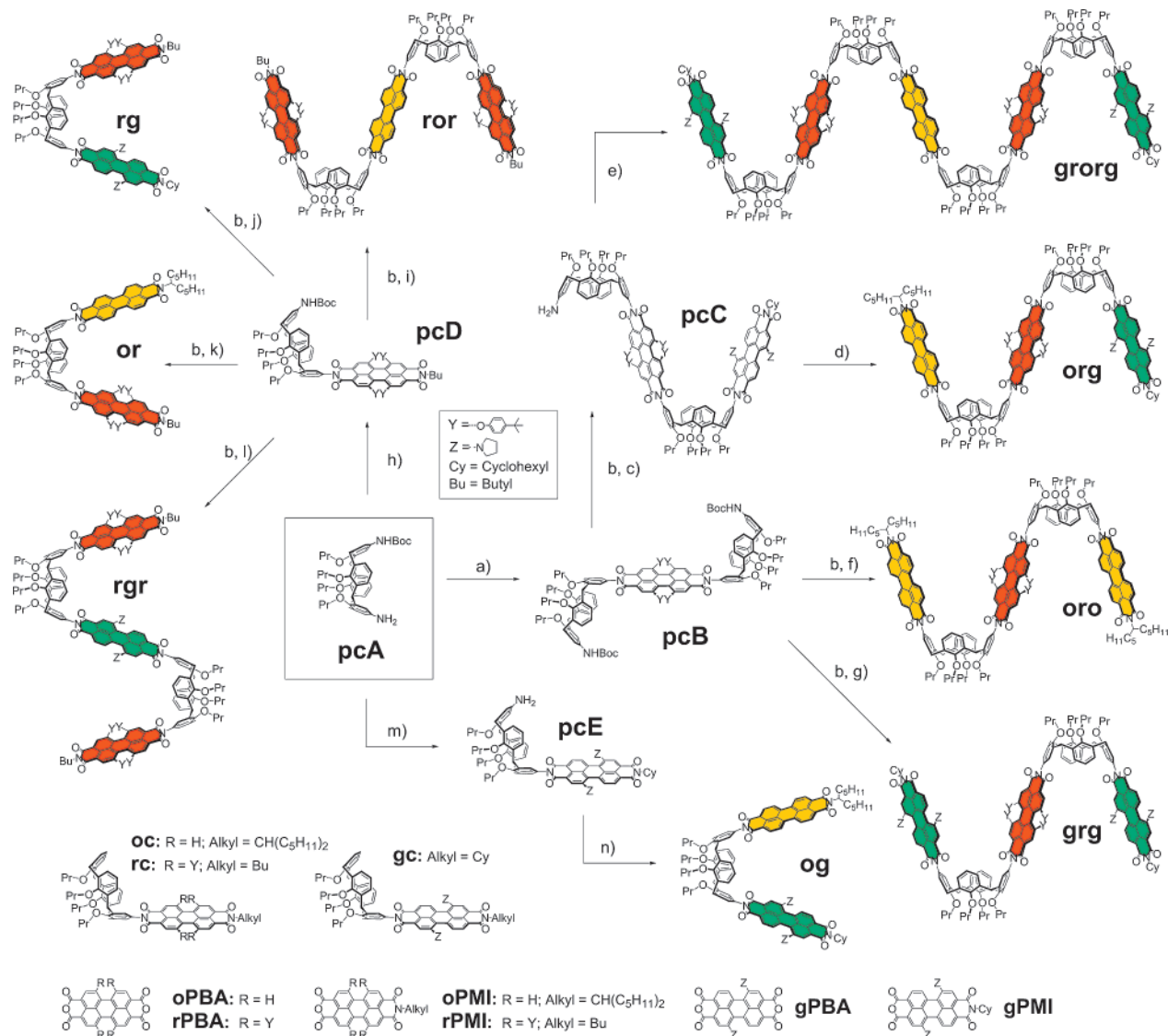
and **grg**, respectively. Furthermore, an array containing an orange, a red, and a green PBI unit has been synthesized and is named as **org**. The array composed of five chromophores, i.e., one orange, two red, and two green PBI units has been presented in our previous communication²⁷ and is denoted here as **grorg**. The monochromophoric references **oc**, **rc**, and **gc** are prepared for the purpose of comparison.

Results and Discussion

Synthesis and Structural Characterization. The syntheses of the investigated perylene bisimide–calix[4]arene arrays are outlined in Scheme 1. The general synthetic strategy is described here exemplarily for the array **org**. A mono-Boc protected calix[4]arene derivative **pcA**, which served as starting material for the present arrays, was first reacted with the red perylene bisanhydride **rpBA** in refluxing toluene/Et₃N to afford the corresponding Boc-protected compound **pcB** (step a in Scheme 1). Deprotection and partial imidization of the latter with the green perylene monoimide **gPMI** in quinoline (catalyst Zn(OAc)₂, 150 °C) yielded the NH₂-functionalized precursor **pcC** (steps b and c) which was further reacted with the orange perylene monoimide **oPMI** (quinoline/Zn(OAc)₂, 165 °C) to obtain the desired array **org** containing three different perylene bisimide chromophores in 49% yield (step d). The other arrays were prepared likewise by successive imidization of the calix[4]arene derivative **pcA** employing the respective desired orange, red, or green perylene monoimide anhydrides or perylene bisanhydrides (details are given in Supporting Information). The arrays **grorg**, **oro**, and **grg** were synthesized by similar procedures as for array **org** from the bis-calix[4]arene substituted intermediate **pcB**, while arrays **ror**, **rg**, **or**, and **rgr** were afforded from the mono-calix[4]arene derivative **pcD** and array **og** from **pcE**. The present synthetic strategy enabled successive incorporation of up to five PBI units in the calix[4]arene scaffold, albeit the overall yield in most cases is relatively low that might be due to the poor solubility of the starting materials and high reaction temperature required for the imidization.

The synthesized perylene bisimide–calix[4]arene arrays were purified by column chromatography (SiO₂) and preparative HPLC (SiO₂, normal phase) and were characterized by ¹H NMR spectroscopy and high-resolution mass spectrometry. The monochromophoric reference compound **rc** was prepared by imidization of 5-monoamino-25,26,27,28-tetrakis(propoxyloxy)-calix[4]arene in refluxing toluene/Et₃N, while the arrays **rg** and **grorg**, and the reference compounds **oc** and **gc** were prepared according to previously reported procedures.^{27,28}

Molecular Structure. To get insights into the 3D structure and the most likely arrangement of the chromophores within the PBI arrays, force field calculations of the bichromophoric arrays **or**, **rg**, and **og** were performed (MacroModel 8.0, potential MMFF). The energetically most favorable structure for **og** is shown in Figure 2, and those for **or** and **rg** are given in Figure S8. These calculated structures, showing a pinched cone conformation with outward-oriented perylene bisimide units, are in good agreement with the crystal structure of an array composed of a calix[4]arene spacer and two red perylene bisimides,²⁹ and also with the structural features of recently investigated naphthalene imide functionalized calix[4]arenes.²⁵ Thus, cofacial orientation of the perylene bisimide chromophores bearing different types of core-substituted PBI units is not preferred in calix[4]arene scaffolds. The molecular structure of compound **or** reveals a center-to-center distance between the orange and the red chromophoric units of $r = 19.9$ Å. The angles of the

SCHEME 1: Synthetic Routes^a and Chemical Structures of PBI–calix[4]arene Arrays Studied Here

^a Reagents and conditions (for steps a-c, e, h and j, see also ref 27): (a) **rPBA**, Et₃N, toluene, reflux, yield 10%; (b) **CF₃COOH**, CH₂Cl₂, rt; (c) **gPMI**, Zn(OAc)₂, quinoline, 150 °C, yield 17% over two steps; (d) **oPMI**, Zn(OAc)₂, quinoline, 165 °C, yield 49%; (e) **oPBA**, Zn(OAc)₂, quinoline, 165 °C, yield 18%; (f) **oPMI**, Zn(OAc)₂, quinoline, 175 °C, yield 38% over two steps; (g) **gPMI**, Zn(OAc)₂, quinoline, 140 °C, yield 18% over two steps; (h) **rPMI**, Et₃N, toluene, reflux, yield 23%; (i) **oPBA**, Zn(OAc)₂, quinoline, 160 °C, yield 35% over two steps; (j) **gPMI**, Zn(OAc)₂, quinoline, 160 °C, yield 28% over two steps; (k) **oPMI**, Zn(OAc)₂, quinoline, 170 °C, yield 23% over two steps; (l) **gPBA**, Zn(OAc)₂, quinoline, 160 °C, yield 30% over two steps; (m) **gPMI**, Zn(OAc)₂, quinoline, 130 °C, yield 14%; (n) **oPMI**, Zn(OAc)₂, quinoline, 155 °C, yield 23%.

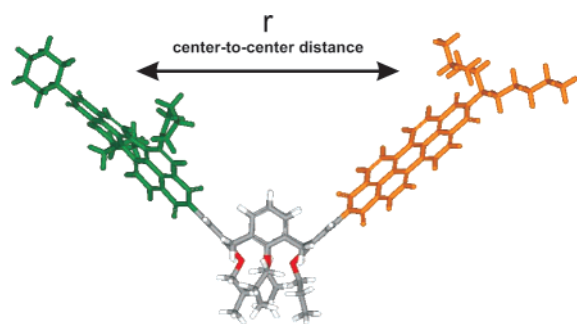


Figure 2. Side view of the molecular structure obtained from force field calculations (Macromodel 8.0, potential MMFF) of compound **og**. PBI chromophores are shown in orange and green color for clarity.

transition dipole moments of the S₀–S₁ transitions (along the N–N-axis of the PBI chromophore) have been determined for **or** as $\Theta_D = 44.1^\circ$ and $\Theta_A = 43.1^\circ$ that denote the angle between the emission transition dipole moment of the donor or acceptor

dye and the vector joining the donor and acceptor units, respectively. The arrays **rg** and **og** show very similar structural features with *r* values around 20 Å and similar Θ_D and Θ_A values.

Obviously, the estimated center-to-center distance *r* and the angles Θ_D and Θ_A do not substantially change upon variation of the PBI building blocks. Hence, within these arrays the individual building blocks can be replaced by each other without affecting the overall geometric arrangement of the supramolecular system, a design principle which is reminiscent of the construction of several natural and synthetic biomacromolecules.³⁰ The energy gradients within the array are controlled by the optical properties of the respective PBI units that are imparted by the electron-donating bay substituents, leading to bathochromic shifts of the absorption maxima. Similar fine-tuning of optical properties has also been found for the related chromophore class of naphthalene bisimide dyes.³¹ Varied absorption and emission properties can also be achieved by extension of the chromophoric π -system, leading, for example,

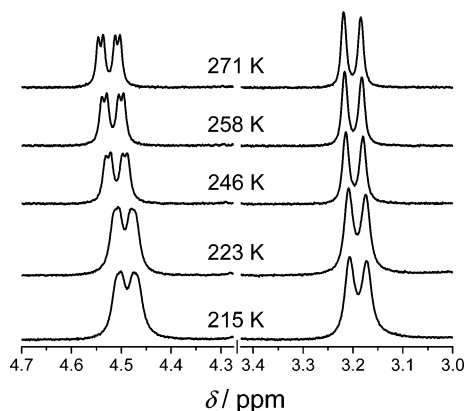


Figure 3. Sections of variable temperature ^1H NMR spectra (400 MHz, in CDCl_3) of array **og** showing the Ar- CH_2 -Ar protons of the calix[4]-arene moiety. Temperature is indicated above the respective spectrum.

in the case of perylene bisimides to the higher homologues terrylene and quaterrylene dyes.³² Building blocks obtained in this manner (here terrylene and quaterrylene dyes), however, differ substantially in length and therefore would not maintain the overall geometry of the supramolecular array owing to the varied dimensions of the individual chromophoric units.

Temperature-Dependent ^1H NMR Studies. To explore the preferred conformation in solution, variable temperature ^1H NMR measurements were performed for the arrays **or**, **rg**, and **og** in the temperature range from 271 to 213 K.

In ^1H NMR spectra of these dyads at room temperature only one set of signals for the Ar- CH_2 -Ar protons of the calix[4]-arene moiety is observed, as exemplarily shown for **og** in Figure 3 (see Figure S9 for **or** and **rg**), although, in principle, two pinched cone conformations of the calix[4]arene unit are possible: One conformation with the PBI residues pointing away from each other (zigzag conformation) and the other one with the PBI units bent toward each other (stacked conformation). Slow interconversion of these two populated conformations would lead to two sets of signals. The observation of only one set of signals in the ^1H NMR spectra of **or**, **rg**, and **og**, respectively, may be rationalized as follows: Either the interconversion between the two possible pinched cone conformations is fast on the NMR time scale, so that the observed spectra correspond to the weighted average of the signals, or this process is such slow on the NMR time scale that the population of one of the two possible pinched cone conformations is too low in concentration to be detected by NMR spectroscopy. Lowering the temperature to around 215 K did not result in any significant change in the ^1H NMR spectra of the arrays **or**, **rg**, and **og**, suggesting that the observed spectra correspond to the prevalence of a single cone conformation within the whole temperature range applied (see Figure 3). Apparently, the population of the second pinched cone conformer is too low to allow its detection by ^1H NMR spectroscopy. Taking into account that the proton resonances of the perylene bisimide units experience negligible shifts (as one would expect by aromatic ring currents in a stacked geometry) compared to those of the reference compounds **oc**, **rc**, and **gc**, and in corroboration with the results from molecular modeling, it can be concluded that also in solution the pinched cone conformation with the outward-oriented perylene bisimide residues prevails. These findings are in good accordance with a detailed study on the conformational properties of calix[4]arenes bearing two PBI dyes in different solvents.²⁹ Further support for the above-mentioned conclusion is given by the excellent agreement of the experimentally obtained rate constants with those calculated according to the

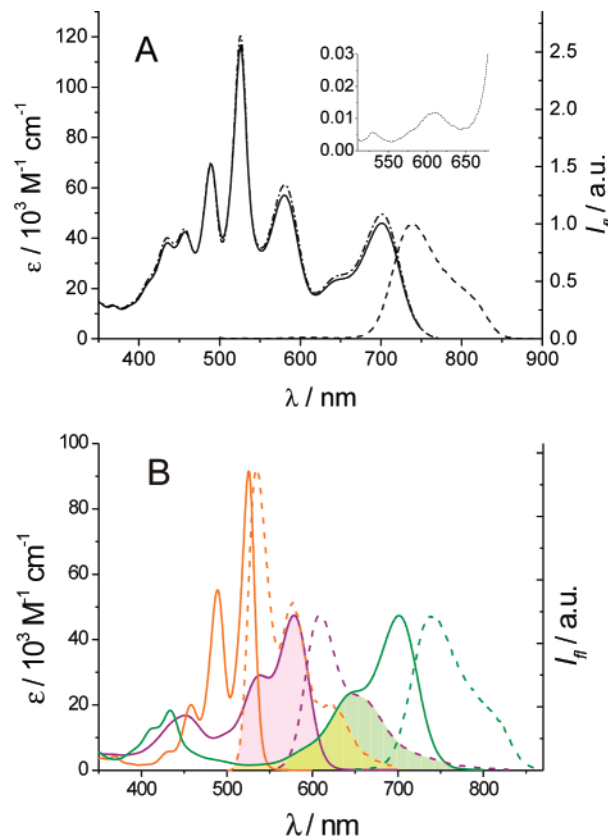


Figure 4. (A) UV/vis absorption (solid line), calculated UV/vis absorption (dash-dotted line; from $\epsilon(\text{oc}) + \epsilon(\text{rc}) + \epsilon(\text{gc})$) and fluorescence emission spectra (dashed line; $\lambda_{\text{ex}} = 490$ nm) of array **og** in CH_2Cl_2 . Inset: Magnification of the fluorescence emission spectrum in the range of 510 to 680 nm. (B) UV/vis absorption (solid lines) and fluorescence emission spectra (dashed lines) of compounds **oc** (orange), **rc** (violet), and **gc** (green). For comparison, the spectral overlap for the respective dye units is highlighted by shading for the donor-acceptor pairs orange-red (violet area), red-green (yellow-green area), and orange-green (yellow area). All spectra are taken in CH_2Cl_2 .

Förster theory, with the rate of energy transfer being strongly dependent on the center-to-center distance r (for details see below).

Optical Properties. The optical properties of the newly synthesized PBI-calix[4]arene arrays were investigated by UV/vis absorption and steady-state fluorescence emission spectroscopy at room temperature. The spectra of the array **org** are shown exemplarily in Figure 4A and those of the monochromophoric references **oc**, **rc**, and **gc** are depicted in Figure 4B. Optical spectra of further arrays are given in the Supporting Information (Figures S10–S12), and the optical data are collected in Table 1. For all the investigated arrays, neither additional absorption nor emission bands emerged, indicating no significant ground state interaction between the chromophores. Hence, the absorption properties of the present arrays are determined by the individual absorption patterns of the parent chromophoric units. For instance, the UV/vis absorption spectrum of array **org** (Figure 4A) shows the characteristic maxima of the containing PBI chromophoric units, i.e., of orange (at 527 and 489 nm), red (at 580 nm), and green PBI (at 701 nm), and the calculated spectrum obtained by summation of the absorption spectra of the respective reference compounds resembles the measured one. Likewise, for all other arrays similar UV/vis absorption features composed from superposition of the individual PBI chromophores are observed (Figures S10–

TABLE 1: Optical Properties of PBI-calix[4]arene Arrays in CH₂Cl₂^a

cmpd	UV/vis absorption						fluorescence emission			
	orange PBI		red PBI		green PBI		λ_{max} (nm)	Φ_{fl} ($\lambda_{\text{ex}} = 450$ nm)	Φ_{fl} ($\lambda_{\text{ex}} = 560$ nm)	Φ_{fl} ($\lambda_{\text{ex}} = 615$ nm)
	λ_{max} (nm)	ϵ (M ⁻¹ cm ⁻¹)	λ_{max} (nm)	ϵ (M ⁻¹ cm ⁻¹)	λ_{max} (nm)	ϵ (M ⁻¹ cm ⁻¹)				
oc ^b	526	91600					535	0.03		
rc			578	47400			608		0.80 ^c	
gc ^d					701	47300	742	0.20		
or	526	107900	579	46200			608 ^e	0.72	0.74	
oro	526	194900	580	50300			611 ^e	0.72	0.70	
ror	527	135000	578	91600			608 ^e	0.73	0.71	
rg ^d			580	50800	701	44600	738 ^f	0.19	0.18	0.21
rgr			579	93700	703	43700	739 ^f	0.19	0.21	0.22
grg			580	61300	701	84800	738 ^f	0.19	0.18	0.17
og	525	89600			700	45200	741 ^e	0.12		0.25
org	527	116800	580	57100	701	46000	737 ^e	0.16	0.18	0.18
grorg ^d	527	127900	581	97600	701	77100	739 ^e	0.17	0.14	0.15

^a All spectra were recorded at room temperature. ^b See ref 28, values are given for comparison. ^c $\lambda_{\text{ex}} = 550$ nm. ^d See ref 27, values are given for comparison. ^e $\lambda_{\text{ex}} = 490$ nm. ^f $\lambda_{\text{ex}} = 560$ nm.

S12). Upon photoexcitation of **org** at $\lambda_{\text{ex}} = 490$ nm (almost exclusive absorption of the orange PBI unit) fluorescence emission of the green PBI chromophore at 737 nm is observed, indicating efficient energy transfer between the chromophoric units. The spectrum in Figure 4A (inset) also shows very weak concomitant fluorescence emission from the red PBI unit at 610 nm. Similar behavior is also observed for arrays **rg**, **rgr**, and **grg**, where upon excitation in the red PBI unit at 560 nm almost exclusive fluorescence emission at around 738 nm is detected, again along with a very weak concomitant emission from the red PBI unit at around 610 nm (see Figure S12). Upon photoexcitation of the arrays **or**, **oro**, and **ror** at 490 nm (almost exclusively in the orange PBI) solely emission of the red PBI at around 608 nm, and no concomitant emission from the orange PBI, is observed (see Figures S10 and S11). Furthermore, fluorescence excitation spectra of arrays **or**, **oro**, and **ror** were recorded ($\lambda_{\text{det}} = 700$ nm; exclusive detection in the emission of the red PBI) in which all UV/vis absorption bands, including those of the orange chromophoric unit (here being the energy donor), are reproduced. Accordingly, independent of the excitation energy, the lowest excited state located on the red PBI acceptor unit is populated for all three compounds, and thus a nearly quantitative energy transfer from the orange to the red chromophoric units takes place,³³ which is further corroborated by the almost perfect overlap of the fluorescence excitation spectra with the respective UV/vis absorption curves (see Figures S10 and S11).

The fluorescence quantum yields of the arrays were measured for different excitation wavelengths and the values are collected in Table 1. As the data in Table 1 reveal, for all the investigated arrays, except for **og**, the quantum yields are independent of the excitation wavelength within the error range of ± 0.03 and they are in reasonable agreement with the values observed for the respective monochromophoric reference compounds. Thus, the quantum yields of the arrays **or**, **oro**, and **ror** are similar to that of reference **rc** and those of the arrays **rg**, **rgr**, **grg**, **org**, and **grorg** are in good agreement with the value of reference **gc**. In contrast to all other arrays, the quantum yield of **og** is dependent on the excitation wavelength ($\Phi_{\text{fl}} = 0.12$ for $\lambda_{\text{ex}} = 450$ nm and 0.25 for $\lambda_{\text{ex}} = 615$ nm). The value for the excitation at $\lambda_{\text{ex}} = 615$ nm in the green chromophore is in reasonable agreement with that obtained for the green reference **gc** ($\Phi_{\text{fl}} = 0.20$). However, when the array **og** was excited at 450 nm exclusively in the orange PBI, significantly reduced quantum yield of 0.12 was obtained. This indicates that, apart from the

energy transfer from the excited orange to the green PBI chromophore, an additional process, apparently concomitant electron transfer from the attached calix[4]arene unit to the orange PBI moiety,²⁸ takes place that reduces the emission intensity of the green PBI upon excitation at 450 nm (see below).

The above-mentioned results unequivocally confirm efficient energy transfer between the orange and red chromophoric units in arrays **or**, **oro**, **ror** and **org**, **grorg**, as well as between the red and green chromophoric units in arrays **rg**, **rgr**, **grg** and **org**, **grorg**, and also, but to a lesser extent, in **og** between the orange and the green chromophoric unit. The significant emission of the arrays containing the orange PBI dye upon excitation at $\lambda_{\text{ex}} = 490$ nm (excitation almost exclusively in the orange chromophore) is particularly impressive because the respective reference compound **oc** is almost nonfluorescent. In our recent work, the fluorescence quenching mechanism has been investigated in detail and could be attributed to a photoinduced electron transfer (PET) from the electron-rich calix[4]arene substituents to the electron-poor orange PBI unit with a rate constant of about $3.1 \times 10^{10} \text{ s}^{-1}$ in CH₂Cl₂ for compound **oc**.²⁸ Thus, the energy transfer process from the orange PBI to the adjacent red PBI in array **org**, and in all other systems containing orange and red chromophoric units, has to be significantly faster than the fluorescence quenching by PET processes from the neighboring calix[4]arene unit (see below).

Femtosecond Transient Absorption Spectroscopy. The excited-state properties of the present calix[4]arene–PBI arrays have been investigated by femtosecond transient absorption spectroscopy, and the results for the array **org** are described here in detail as a representative example. The obtained spectra and respective single line kinetics for **org** in CH₂Cl₂ are depicted in Figure 5. The spectra of the remaining arrays and their single line kinetic traces are given in Supporting Information (Figures S13, S14, and S18).

Upon photoexcitation of **org**, containing an orange, a red, and a green chromophoric unit, the immediate formation of strong negative signals at 460, 490, 531, and 585 nm are observed (that are assigned to the combined ground state bleaching and stimulated emission signals from the red and the orange chromophore),^{34,7d} together with a strong positive band centered at 715 nm due to the overlapping excited singlet state absorptions of the orange and red PBI units at that wavelength. These spectral characteristics change very rapidly during further temporal evolution of the spectra to finally result in the concomitant rise of the broad negative band centered at 730

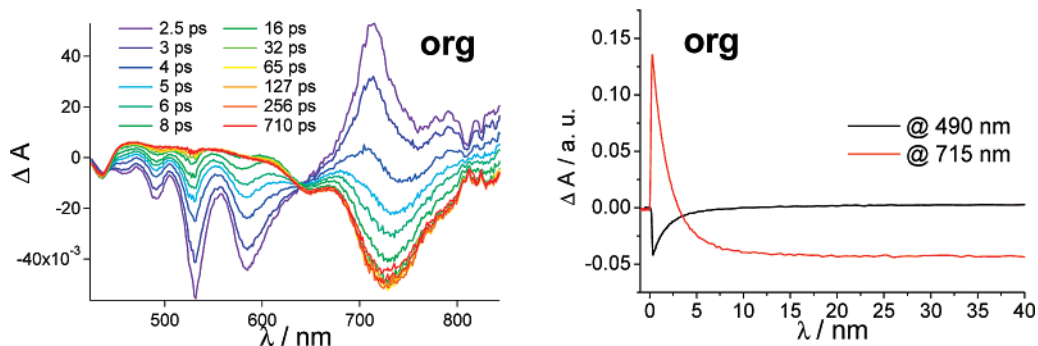


Figure 5. Femtosecond transient absorption spectra and corresponding time delays in CH_2Cl_2 after photoexcitation of the array **org** at 530 nm (left panel). Kinetic profiles (right panel) of the transient absorption spectra measured at 490 nm (black line) and 715 nm (red line).

nm together with a small bleach signal at 435 nm that are attributed to the spectral features of the green chromophore.^{35,36} No recovery of the ground state was observed within the instrument's time frame as the excited-state lifetime of the green PBI chromophore is in the nanosecond time regime. These results clearly reveal the depopulation of the singlet excited-state of the orange as well as the red perylene bisimide unit and provide unambiguous evidence for the very efficient energy transfer process to the green chromophore expressed by the population of the singlet excited-state of the green PBI unit in **org**. Femtosecond transient absorption spectra of all other arrays in CH_2Cl_2 together with a detailed discussion of the spectra of bichromophoric arrays **or**, **rg**, and **og** are given in Supporting Information (Figures S13 and S14 and pages S20–S21). These spectra reveal an efficient energy transfer from the orange to the red PBI unit in arrays **or**, **oro**, and **ror**, as well as from the red to the green PBI in arrays **rg**, **rgr**, and **grg**.³⁵ Furthermore, the rapid energy transfer between the orange and the green chromophoric units is unequivocally confirmed for compound **og** (see Figures S13 and S14 and discussion on pages S20–S21 in Supporting Information). However, for array **og**, the amplitude for the bleaching of the green PBI chromophore at 730 nm remains rather small (compared with that of **rg**) due to the formation of radical anions of the orange PBI unit (that absorbs at about 700 nm)²⁸ by the competing PET process from the electron-rich calix[4]arene to the electron-poor orange PBI (Figures S13 and S14). Similar band shapes and positions as well as an identical spectral evolution as for array **org** (Figure 5, left panel) are also observed in the femtosecond transient absorption spectra of the array **gorg** (Figure S13), again confirming very efficient energy transfer process from the orange as well as the red perylene bisimide unit to the green chromophore.

The energy transfer processes are also evident from the kinetic profiles of the transient absorption data of the array **org** (Figure 5, right panel): the rise (trace at 715 nm, red line) observed for the green perylene bisimide emission (here: the acceptor dye) is almost identical to the decay (trace at 490 nm, black line) of the quenched orange perylene bisimide emission (here: the donor dye). For all other arrays, similar complementary decay and rise profiles were found (for kinetic profiles, see Figure S18). The evaluation of the single line kinetics, however, turned out to be complex especially for the arrays **org** and **gorg**, since a variety of different processes takes place after photoexcitation. Therefore, the kinetic profiles of all systems were further investigated in detail by means of global and target analysis and are discussed below.

Global and Target Analysis. The femtosecond transient absorption data-matrices were analyzed with spectrotemporal parametrization, an advanced global and target analysis method that has been extensively used to elucidate photoinduced processes in nonbiological as well as in complex biological systems

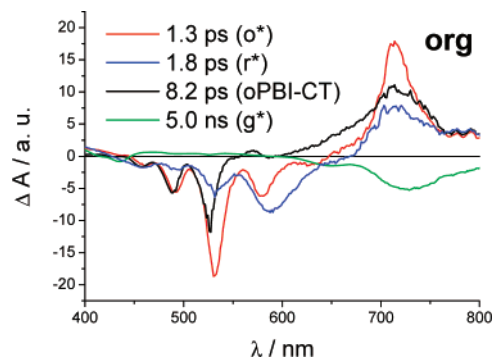


Figure 6. Species-associated difference spectra (SADS) obtained from the target analysis of the femtosecond transient absorption data of array **org** by employing the kinetic scheme depicted in Figure 7A. Processes after photoexcitation at 530 nm are shown with the species: o^* (red line), r^* (blue line), oPBI-CT (black line), and g^* (green line). Features due to Raman scattering and fast solvent reorganization processes were omitted for clarity.

such as photosystems.³⁷ As a final result, the so-called species associated difference spectra (SADS) are obtained, which provide the lifetimes and the true spectra of the individual excited-state species as well. An elaborate example on spectrotemporal parametrization for the calix[4]arene–PBI conjugate **oc** with further details of the method has been published recently.²⁸

As a representative example, the SADS of array **org** resulting from the global fit of the data are shown in Figure 6. For further details on the data analysis and a detailed discussion of the SADS of array **og**, as well as for selected traces and fits, see Supporting Information (Figures S20 and S21 and pages S26–S28). The lifetime values obtained from the data analysis of the processes after photoexcitation are summarized in Table 2 (for the related rate constants, see Table S1 in Supporting Information). For the fitting procedure, a specific model of the excited-state processes was applied according to the energy level diagram depicted in Figure 7A, where a competitive charge transfer (CT) state is formed by electron transfer from the calix[4]arene moiety to the orange PBI unit.²⁸ For array **org**, the initial spectrum in Figure 6 (red line) shows the transient absorption features of the excited singlet state of the orange PBI chromophore.^{28,38} This spectrum is decaying with 1.3 ps via two deactivation pathways: (i) The energy transfer process from the orange to the red PBI unit (for the formation of the excited state of red PBI, see blue spectrum in Figure 6) with 89% amplitude and (ii) the formation of a CT state of the calix[4]arene–orange PBI subunit with 11% amplitude (black line in Figure 6).³⁹ The latter reveals precisely the spectral features of a charge transfer state as the stimulated emission at 580 nm is not observed any longer and the band at around 700 nm is significantly broadened. From this clear spectral evidence,

TABLE 2: Lifetimes in CH₂Cl₂ Obtained from the Global and Target Analysis of the Experimental Data Employing the Model Depicted in Figure 7A

cmpd	(o,r) _{solv} ^{*b}	lifetime τ (ps) ^a						
		ET o* \rightarrow r*	ET r* \rightarrow g*	ET o* \rightarrow g*	CT to (oPBI) ⁻	(oPBI) ⁻	r* \rightarrow r	g* \rightarrow g
or	0.25	1.6			8.2	6.6	5000 ^c	
oro	0.25	1.6			7.5	6.6	3400 ^c	
ror	0.3	0.8			3.0	5.7	3300 ^c	
rg	0.3		2.5					3300
rgr	0.3		2.6					1800
grg	0.2		1.2					900
org	0.2	1.4	1.8		12.0	8.2		5000
grorg	0.2	0.6	2.9		4.5	9.0		2800
og	0.2			6.7	10.8	8.6		3800
oc ^d					32.0	10.0		

^a Relative precision of the lifetimes is 10%, except for lifetimes in the ns time range which are less accurate owing to the 1 ns time frame of the experiment and, thus, represent lower limits. For the related rate constants, see Table S1 in Supporting Information. ^b See ref 38. ^c Note, that for the relaxation of r* also minor components of several hundred picoseconds have been observed which can be attributed to conformational changes of the red perylene bisimide dye (see ref 35). ^d See ref 28.

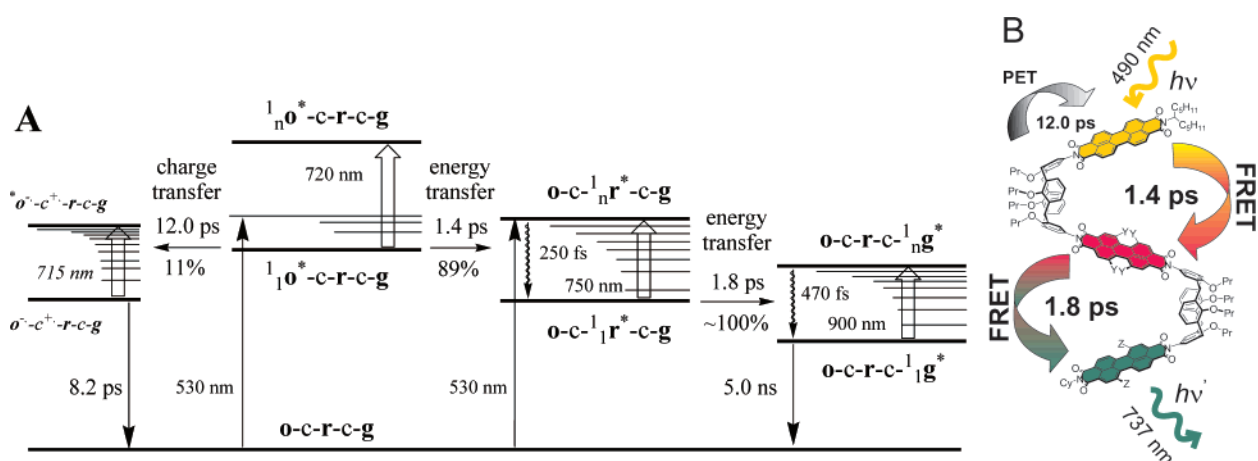


Figure 7. Energy level diagram (A) showing energy and electron-transfer pathways in CH₂Cl₂ obtained with global and target analysis, together with the main decay times corresponding to the respective states for array **org**. Schematic representation (B) for the processes occurring in **org** upon photoexcitation. Note that the lifetimes in the ns time range are less reliable due to the 1 ns time frame of the experiment and, thus, represent lower limits. All other PBI-calix[4]arene arrays have been analyzed similarly as in the case of **org** and the obtained lifetimes are summarized in Table 2 (related rate constants are given in Table S1 and additional energy level diagrams for arrays **or**, **rg**, and **og** are shown in Figure S22).

the formation of a charge-separated state involving the formation of the orange PBI monoanion can be concluded. A similar competitive pathway via formation of a CT state of the calix[4]arene-PBI subunit was already observed for the orange reference compound **oc**.²⁸ The latter charge-transfer state (black line in Figure 6) recombines with 8.2 ps, whereas the excited-state of the red PBI (blue line in Figure 6) decays further with 1.8 ps to form the final green SADS showing a lifetime of 5.0 ns which was assigned to decay of the excited-state of the green PBI unit.³⁶ The latter value is in reasonable agreement with the lifetime of free green PBIs reported in literature.⁸ However, it has to be noted that the longest lifetime values are prone to large errors due to the time frame of the instrument of 1 ns and therefore differ from the values obtained from time-resolved emission experiments.^{27,28} However, they reveal the correct order of magnitude of the lifetimes of the reference chromophores and represent their lower limits. These findings provide unambiguous evidence for sequential energy transfer from the orange to the red and from the red to the green PBI moiety in array **org**. Direct excitation energy deactivation from the orange to the green chromophore was not observed, which is most likely owing to the less favorable spectral overlap of these two dye units.

The observed directional, sequential energy transfer in array **org** from the orange to the red and from the red to the green PBI unit shows a remarkably high overall efficiency of about 89%. This is especially striking because an additional very fast competitive PET process between the linking calix[4]arene units and the orange perylene bisimide chromophore occurs. However, the energy transfer process turns out to be much more efficient and, accordingly, these zigzag-type dye arrays can even harvest the photons absorbed by the orange perylene bisimide dye unit, despite almost nonfluorescent nature of the energy donor subunit, i.e., the parent calix[4]arene-*perylen*e bisimide conjugate **oc**.²⁸ Hence, the present array **org** reveals a much higher overall energy transfer efficiency than observed for many other perylene bisimide based light-harvesting systems known in literature, where significant loss (50% and more) of the excitation energy is caused by undesired competitive PET processes.^{7a-c}

The lifetimes for all other PBI-calix[4]arene arrays (corresponding rate constants are given in Table S1), are very similar to those mentioned above. A component due to energy transfer from the orange to the red PBI unit with values ranging from $\tau = 0.6$ ps (for **grorg**) to $\tau = 1.6$ ps (for **or** and **oro**) as well as a component due to energy transfer from red to green with values ranging from $\tau = 1.2$ ps (for **grg**) to $\tau = 2.9$ ps (for **grorg**). The formation of the CT state of the calix[4]arene-

TABLE 3: Evaluation of Selected Time-resolved Photophysical Properties of Calix[4]arene–PBI Arrays^a According to the Förster Theory

compd	$k_{\text{ET}}(\text{obs})^b$ (10^{11} s^{-1})	E_{ET}^b	E_{CT}^c	$J(\lambda)$ ($\text{M}^{-1}\text{cm}^{-1}\text{nm}^4$)	R_0 (\AA)	$k_{\text{ET}}(\text{calcd})$ (10^{11} s^{-1})
or	6.4	0.84	0.16	2.53×10^{15d}	70.8	5.9
oro	6.3	0.82	0.18			
ror	12.6	0.79	0.21			
rg	4.0	~1.00	~0.00	3.43×10^{15e}	74.5	4.0
rgr	3.9	~1.00	~0.00			
grg	8.5	~1.00	~0.00			
org	7.1	0.89	0.11			
grorg	15.8	0.88	0.12			
og	1.5	0.62	0.38	8.08×10^{14f}	58.7	1.9

^a All spectra were recorded at room temperature in CH_2Cl_2 . ^b Rate constants and efficiency values are given for the energy transfer processes from the orange to the red PBI unit in arrays **or**, **oro**, **ror**, **org**, and **grorg**, and from the red to the green PBI unit for **rg**, **rgr**, and **grg**. ^c Efficiency values are given for the charge-transfer processes from the calix[4]arene moiety to the orange PBI unit in arrays **or**, **oro**, **ror**, **org**, and **grorg**, and to the red PBI unit in arrays **rg**, **rgr**, and **grg**. ^d Calculated from normalized fluorescence emission spectrum of reference compound **oc** and UV/vis absorption spectrum of compound **rc**. ^e Calculated from normalized fluorescence emission spectrum of **rc** and UV/vis absorption spectrum of **gc**. ^f Calculated from normalized fluorescence emission spectrum of **oc** and UV/vis absorption spectrum of **gc**.

orange PBI subunit is also observed as a competitive side process with values ranging from $\tau = 3.0$ ps (for **ror**) to $\tau = 12.0$ ps (for **og**). The latter CT state shows lifetimes with values ranging from $\tau = 5.7$ ps (for **ror**) to $\tau = 9.0$ ps (for **grorg**). Furthermore, the lifetimes (representing lower limit values due to the time frame of the experiment) of the final long-living excited acceptor states of the respective PBI unit are also given in Table 2. Notably, for systems containing two acceptors like in arrays **ror** and **grg**, the decay time of the excited energy donor unit (orange PBI in **ror** and red PBI in **grg**) is further reduced by half and the respective rate constant doubles, whereas for arrays containing just one acceptor but two donor units like in arrays **rgr** and **oro**, no such effects are observed (see Table 1).

Furthermore, the impact of the solvent polarity on the transient absorption spectra and the energy transfer rates has been studied for the three systems **or**, **rg**, and **og**. As expected, the energy transfer rates and the kinetic profiles differ only slightly in solvents of different polarity which is in agreement with the solvent independency usually observed for Förster-type resonance energy transfer (for a discussion, see pages S31 and S33 in Supporting Information).⁴⁰ The femtosecond transient absorption data and representative kinetic traces are shown in Figures S15–S19, and the lifetime values obtained from the global and target analysis are summarized in Table S2.

From the femtosecond transient absorption results (given in Table 2 and Table S1), energy transfer rates k_{ET} for the energy transfer from the orange to the red PBI unit (for **or**), from the red to the green PBI moiety (for **rg**), and from the orange to the green PBI chromophore (for **og**) can be obtained (see Table 3). Based on these rate constants, the efficiency of the energy transfer process E_{ET} as well as the efficiency of the competitive charge-transfer process E_{CT} can be calculated⁴¹ and, accordingly, a value of $E_{\text{ET}} = 0.84$ is obtained for the efficiency of the energy transfer process from the orange to the red PBI unit in array **or**. Likewise, the arrays **oro**, **ror**, **org**, and **grorg** reveal very similar energy transfer efficiencies (Table 3). Notably, the energy transfer efficiencies for these arrays are a little bit lower than expected from their very high rate constants. However, due to the competitive charge transfer state formation, which

is also a pretty fast process (the respective rate constants range from $k_{\text{CT}} = 0.92 \times 10^{11} \text{ s}^{-1}$ for **og** to $k_{\text{CT}} = 3.3 \times 10^{11} \text{ s}^{-1}$ for **ror**), slightly reduced energy transfer efficiency is reasonable. The efficiency of the energy transfer process from the red to the green PBI unit results in a E_{ET} value of about 1.00 for all the three arrays **rg**, **rgr**, and **grg**, respectively, as no formation of a competitive charge transfer state consisting of the red PBI monoanion and the cation of the calix[4]arene unit has been observed for the deactivation of the red excited-state in these arrays.⁴² The smallest E_{ET} value (0.62) is obtained for the energy transfer process from the orange to the green PBI unit in **og**, thus, with the orange-green couple **og** the critical limit for efficient energy transfer processes in PBI arrays is given. On the one hand, the charge-transfer process from the electron-rich calix[4]arene unit to the electron deficient orange PBI chromophore is very efficient and, on the other hand, for the orange-green donor–acceptor pair, the smallest extent of spectral overlap is given (see Figure 4B). As a consequence, the energy transfer between the two chromophoric units is less efficient and the competing charge-transfer process becomes more pronounced. Assuming a fluorescence resonance energy transfer (FRET), the experimentally obtained energy-transfer rates can be compared to the rate constants calculated by employing the Förster theory. Accordingly, the transfer rate depends on following factors: The extent of spectral overlap of the emission spectrum of the donor with the absorption spectrum of the acceptor $J(\lambda)$ (see Figure 4B), the quantum yield of the donor in the absence of the acceptor Φ_{D} , the relative orientation of the donor and acceptor transition dipoles (described by the orientation factor κ^2), and the distance between the donor and acceptor molecules.⁴³ The thus obtained values are collected in Table 3 (further details on the calculation are given in Supporting Information, page S33). Typical values for the Förster distance reported in the literature range from 10 to 80 \AA which is in agreement with the obtained data.⁴⁴ Furthermore, the rate of energy transfer from a donor to an acceptor can be afforded from the Förster theory employing the center-to-center distance r from the molecular modeling structures depicted in Figure 2. This leads to the calculated values for the energy transfer rate of $k_{\text{ET}} = 5.9 \times 10^{11} \text{ s}^{-1}$ for **or**, $4.0 \times 10^{11} \text{ s}^{-1}$ for **rg**, and $1.9 \times 10^{11} \text{ s}^{-1}$ for **og** which excellently corroborate with the experimentally obtained rate constants of these arrays (see Table 3). Thus, the molecular structure obtained from modeling (Figure 2) provided the correct spatial orientation of the chromophores to explain the energy transfer rates by the Förster theory (see eqs S1 and S2 in Supporting Information, page S33) as the rate of energy transfer is inversely proportional to r^6 and thus depends strongly on the center-to-center distance r of the donor and acceptor transition dipoles. Hence, any phenomenon affecting the distance r will also influence the transfer rate to a large extent. With such an excellent agreement of experimentally observed and theoretically calculated values for the rate constants by employing the r value related to the zigzag pinched cone conformation (i.e., the pinched cone conformation with the PBI residues pointing away from each other), spectroscopic evidence for the prevalence of the latter conformation is provided. Accordingly, our time-resolved spectroscopic results support the absence of the stacked pinched cone conformation (with co-facial orientation of the PBI units), as the center-to-center distance in that case would be substantially smaller and the values of experimentally and theoretically obtained rate constants would differ to a large extent.

Conclusions

Calix[4]arene scaffolds have been applied to organize perylene bisimide chromophores in zigzag-type arrangements providing defined distances and angles between the perylene bisimide chromophores. Arrays constructed in such way possess the characteristic feature that the individual chromophoric building blocks can be easily replaced by each other as well as their optical properties can be fine-tuned without influencing the overall geometric arrangement of the supramolecular system. Owing to the excellent spectral overlap of orange and red as well as of red and green perylene bisimide chromophores, the **org** triad displays very fast directional energy transfer leading to the population of the excited green PBI in less than 4 ps and with 89% efficiency. For comparison, in the absence of the red “mediator” chromophore, a slower (7 ps) and less efficient (62%) energy transfer process is observed for the **og** dyad. Therefore, these zigzag-type dye arrays can even harvest the photons absorbed by the orange perylene bisimide dye unit, despite almost nonfluorescent nature of the parent calix[4]arene–perylene bisimide building block **oc**. The zigzag-type arrangement of dyes employed here provided a hitherto unexplored geometry for efficient sequential FRET processes along oligomeric chains with κ^2 values of around 2.3 which compare well with intensively investigated linear arrays (showing values of $\kappa^2 = 4$ or 1). Femtosecond transient absorption spectroscopy provided valuable information on the excited states and global analysis revealed intricate details as the three different PBI chromophores applied here display well separable characteristics. The observed energy transfer processes are in excellent agreement with Förster theory. Stimulated by the fact that such PBI arrays are not only excellent candidates for sequential energy transfer but also enable the formation of long-lived charge separated states,⁴⁵ our next logical approach would be to combine both features in a sequential energy and electron-transfer cascade.

Acknowledgment. We are grateful for financial support to the Deutsche Forschungsgemeinschaft (DFG) (Grant Wu 317/4-1) and the Graduiertenkolleg (GK) 1221 “Control of electronic properties of aggregated π -conjugated molecules”, to the Nederlandse organisatie voor Wetenschappelijk Onderzoek (NWO) for the femtosecond equipment, and to the Universiteit van Amsterdam (UvA). C.H. is thankful to the Fonds der Chemischen Industrie for a Kekulé fellowship. We thank Dr. Volker Böhmer for many helpful discussions on the synthesis and the structural properties of calix[4]arenes.

Supporting Information Available: Synthetic and experimental details of all compounds, femtosecond transient absorption spectra as well as data obtained from global and target analysis. This material is available free of charge via the Internet at <http://pubs.acs.org>

References and Notes

- (1) (a) Huber, R. *Angew. Chem., Int. Ed. Engl.* **1989**, *28*, 848–869. (b) Pullerits, T.; Sundström, V. *Acc. Chem. Res.* **1996**, *29*, 381–389. (c) Hu, X.; Ritz, T.; Damjanović, A.; Autenrieth, F.; Schulten, K. *Q. Rev. Biophys.* **2002**, *35*, 1–62. (d) Cogdell, R. J.; Lindsay, J. G. *New Phytol.* **2000**, *145*, 167–196. (e) Holzwarth, A. R. In *Series on Photoconversion of Solar Energy*; Archer, M. D., Barber, J., Eds.; Imperial College Press: London, U.K., 2002; pp 43–115.
- (2) (a) Hoeben, F. J. M.; Jonkheijm, P.; Meijer, E. W.; Schenning, A. P. H. J. *Chem. Rev.* **2005**, *105*, 1491–1546. (b) Wasielewski, M. R. *Chem. Rev.* **1992**, *92*, 435–461. (c) Gust, D.; Moore, T. A.; Moore, A. L. *Acc. Chem. Res.* **2001**, *34*, 40–48. (d) Adronov, A.; Fréchet, J. M. J. *Chem. Commun.* **2000**, 1701–1710. (e) *Comprehensive Supramolecular Chemistry*; Lehn, J.-M., Atwood, J. L., Davies, J. E. D., MacNicol, D. D., Vögtle, F.,

- Eds.; Pergamon: Oxford, 1996; Vol. 1–11. (f) Wasielewski, M. R. *J. Org. Chem.* **2006**, *71*, 5051–5066. (g) Gust, D.; Moore, T. A.; Moore, A. L. *Acc. Chem. Res.* **1993**, *26*, 198–205. (h) Scandola, F.; Indelli, M. T.; Chiorboli, C.; Bignozzi, C. A. *Top. Curr. Chem.* **1990**, *158*, 73–149. (i) Choi, M.-S.; Yamazaki, T.; Yamazaki, I.; Aida, T. *Angew. Chem., Int. Ed.* **2004**, *43*, 150–158.

(3) *Supramolecular Dye Chemistry*; Würthner, F., Ed.; Topics in Current Chemistry Vol. 258; Springer-Verlag: Berlin, 2005.

(4) (a) Paddon-Row, M. N. In *Stimulating Concepts in Chemistry*; Vögtle, F., Stoddart, J. F., Shibasaki, M., Eds.; Wiley-VCH: Weinheim, Germany, 2000; pp 267–291. (b) Armadori, N. *Photochem. Photobiol. Sci.* **2003**, *2*, 73–87. (c) Barigelletti, F.; Flamigni, L. *Chem. Soc. Rev.* **2000**, *29*, 1–12. (d) Guldí, D. M. *Chem. Soc. Rev.* **2002**, *31*, 22–36. (e) Holten, D.; Bocian, D. F.; Lindsey, J. S. *Acc. Chem. Res.* **2002**, *35*, 57–69. (f) Prodi, A.; Indelli, M. T.; Kleverlaan, C. J.; Alessio, E.; Scandola, F. *Coord. Chem. Rev.* **2002**, *229*, 51–58. (g) Harriman, A.; Sauvage, J.-P. *Chem. Soc. Rev.* **1996**, *25*, 41–48. (h) Nakamura, Y.; Hwang, I.-W.; Aratani, N.; Ahn, T. K.; Ko, D. M.; Takagi, A.; Kawai, T.; Matsumoto, T.; Kim, D.; Osuka, A. *J. Am. Chem. Soc.* **2005**, *127*, 236–246. (i) Balzani, V.; Juris, A. *Coord. Chem. Rev.* **2001**, *211*, 97–115.

(5) For light-harvesting linear arrays containing perylene bisimides, see: (a) Prathapan, S.; Yang, S. I.; Seth, J.; Miller, M. A.; Bocian, D. F.; Holten, D.; Lindsey, J. S. *J. Phys. Chem. B* **2001**, *105*, 8237–8248. (b) Rytbchinski, B.; Sinks, L. E.; Wasielewski, M. R. *J. Am. Chem. Soc.* **2004**, *126*, 12268–12269. (c) Ego, C.; Marsitzky, D.; Becker, S.; Zhang, J.; Grimsdale, A. C.; Müllen, K.; MacKenzie, J. D.; Silva, C.; Friend, R. H. *J. Am. Chem. Soc.* **2003**, *125*, 437–443. (d) Loewe, R. S.; Tomizaki, K.-Y.; Youngblood, W. J.; Bo, Z.; Lindsey, J. S. *J. Mat. Chem.* **2002**, *12*, 3438–3451. (e) Schlichting, P.; Duchscherer, B.; Seisenberger, G.; Basché, T.; Bräuchle, C.; Müllen, K. *Chem. Eur. J.* **1999**, *5*, 2388–2395. (f) Hinze, G.; Haase, M.; Nolde, F.; Müllen, K.; Basché, T. *J. Phys. Chem. A* **2005**, *109*, 6725–6729.

(6) For light-harvesting dendrimers containing perylene bisimides, see: (a) De Schryver, F. C.; Vosch, T.; Cotlet, M.; Van der Auweraer, M.; Müllen, K.; Hofkens, J. *Acc. Chem. Res.* **2005**, *38*, 514–522. (b) Serin, J. M.; Brousmiche, D. W.; Fréchet, J. M. J. *Chem. Commun.* **2002**, 2605–2607. (c) Serin, J. M.; Brousmiche, D. W.; Fréchet, J. M. J. *J. Am. Chem. Soc.* **2002**, *124*, 11848–11849. (d) Gronheid, R.; Stefan, A.; Cotlet, M.; Hofkens, J.; Qu, J.; Müllen, K.; Van der Auweraer, M.; Verhoeven, J. W.; De Schryver, F. C. *Angew. Chem., Int. Ed.* **2003**, *42*, 4209–4214. (e) Weil, T.; Reuther, E.; Müllen, K. *Angew. Chem., Int. Ed.* **2002**, *41*, 1900–1904. (f) Gronheid, R.; Hofkens, J.; Köhn, F.; Weil, T.; Reuther, E.; Müllen, K.; De Schryver, F. C. *J. Am. Chem. Soc.* **2002**, *124*, 2418–2419. (g) Jordens, S.; De Belder, G.; Lor, M.; Schweitzer, G.; Van der Auweraer, M.; Weil, T.; Reuther, E.; Müllen, K.; De Schryver, F. C. *Photochem. Photobiol. Sci.* **2003**, *2*, 177–186.

(7) (a) Sautter, A.; Kaletas, B. K.; Schmid, D. G.; Dobrawa, R.; Zimine, M.; Jung, G.; Van Stokkum, I. H. M.; De Cola, L.; Williams, R. M.; Würthner, F. *J. Am. Chem. Soc.* **2005**, *127*, 6719–6729. (b) You, C.-C.; Hippius, C.; Grüne, M.; Würthner, F. *Chem. Eur. J.* **2006**, *12*, 7510–7519. (c) Flamigni, L.; Ventura, B.; You, C.-C.; Hippius, C.; Würthner, F. *J. Phys. Chem. C* **2007**, *111*, 622–630. (d) Prodi, A.; Chiorboli, C.; Scandola, F.; Iengo, E.; Alessio, E.; Dobrawa, R.; Würthner, F. *J. Am. Chem. Soc.* **2005**, *127*, 1454–1462.

(8) Würthner, F. *Chem. Commun.* **2004**, 1564–1579.

(9) For general examples of linear light-harvesting arrays, see: (a) Zissler, R.; Hissler, M.; El-ghayoury, A.; Harriman, A. *Coord. Chem. Rev.* **1998**, *178–180*, 1251–1298. (b) Aratani, N.; Osuka, A.; Cho, H. S.; Kim, D. *J. Photochem. Photobiol. C* **2002**, *3*, 25–52. (c) Bossart, O.; De Cola, L.; Welter, S.; Calzaferrri, G. *Chem. Eur. J.* **2004**, *10*, 5771–5775. (d) Berglund Baudin, H.; Davidsson, J.; Serroni, S.; Juris, A.; Balzani, V.; Campagna, S.; Hammarström, L. *J. Phys. Chem. A* **2002**, *106*, 4312–4319. (e) Chiorboli, C.; Indelli, M. T.; Scandola, F. *Top. Curr. Chem.* **2005**, *257*, 63–102. (f) Harriman, A.; Zissler, R. *Coord. Chem. Rev.* **1998**, *171*, 331–339. (g) Yang, S. I.; Seth, J.; Balasubramanian, T.; Kim, D.; Lindsey, J. S.; Holten, D.; Bocian, D. F. *J. Am. Chem. Soc.* **1999**, *121*, 4008–4018.

(10) (a) Fujita, M. *Chem. Soc. Rev.* **1998**, *27*, 417–425. (b) Stang, P. J.; Olenyuk, B. *Acc. Chem. Res.* **1997**, *30*, 502–518. (c) Würthner, F.; You, C.-C.; Saha-Möller, C. R. *Chem. Soc. Rev.* **2004**, *33*, 133–146. (d) Slone, R. V.; Benkstein, K. D.; Bélanger, S.; Hupp, J. T.; Guzei, I. A.; Rheingold, A. L. *Coord. Chem. Rev.* **1998**, *171*, 221–243. (e) Amijs, C. H. M.; van Klink, G. P. M.; van Koten, G. *Dalton Trans.*, **2006**, 308–327. (f) Seidel, S. R.; Stang, P. J. *Acc. Chem. Res.* **2002**, *35*, 972–983. (g) M. H. Keefe; K. D. Benkstein; Hupp, J. T. *Coord. Chem. Rev.* **2000**, *205*, 201–228.

(11) For general examples on light-harvesting dendrimers, see: (a) Dirksen, A.; De Cola, L. *C. R. Chimie* **2003**, *6*, 873–882. (b) *Dendritic Molecules: Concepts, Syntheses, Perspectives*; Newkome, G. R.; Moorefield, C. N.; Vögtle, F., Eds.; VCH: New York, 1996. (c) Balzani, V.; Ceroni, P.; Maestri, M.; Saudan, C.; Vicinelli, V. *Top. Curr. Chem.* **2003**, *228*, 159–191. (d) Venturi, M.; Serroni, S.; Juris, A.; Campagna, S.; Balzani, V. *Top. Curr. Chem.* **1998**, *197*, 193–228. (e) Hahn, U.; Gorka, M.; Vögtle, F.; Vicinelli, V.; Ceroni, P.; Maestri, M.; Balzani, V. *Angew. Chem., Int.*

- Ed. **2002**, 41, 3595–3598. (f) Balzani, V.; Campagna, S.; Denti, G.; Juris, A.; Serroni, S.; Venturi, M. *Acc. Chem. Res.* **1998**, 31, 26–34.
- (12) Examples for supramolecular systems containing π - π -stacked perylene bisimides: (a) Würthner, F.; Thalacker, C.; Sautter, A.; Schärfl, W.; Ibach, W.; Hollricher, O. *Chem. Eur. J.* **2000**, 6, 3871–3886. (b) Peeters, E.; van Hal, P. A.; Meskers, S. C. J.; Janssen, R. A. J.; Meijer, E. W. *Chem. Eur. J.* **2002**, 8, 4470–4474. (c) Würthner, F.; Chen, Z.; Dehm, V.; Stepanenko, V. *Chem. Commun.* **2006**, 1188–1190. (d) Hernandez, J.; De Witte, P. A. J.; Van Dijk, E. M. H. P.; Korterik, J.; Nolte, R. J. M.; Rowan, A. E.; Garcia-Parajó, M. F.; Van Hulst, N. F. *Angew. Chem., Int. Ed.* **2004**, 43, 4045–4049. (e) Beckers, E. H. A.; Meskers, S. C. J.; Schenning, A. P. H. J.; Chen, Z.; Würthner, F.; Marsal, P.; Beljonne, D.; Cornil, J.; Janssen, R. A. J. *J. Am. Chem. Soc.* **2006**, 128, 649–657.
- (13) (a) Talukdar, P.; Bollot, G.; Mareda, J.; Sakai, N.; Matile, S. *J. Am. Chem. Soc.* **2005**, 127, 6528–6529. (b) Bhosale, S.; Sisson, A. L.; Talukdar, P.; Fürstenberg, A.; Banerji, N.; Vauthey, E.; Bollot, G.; Mareda, J.; Röger, C.; Würthner, F.; Sakai, N.; Matile, S. *Science* **2006**, 313, 84–86.
- (14) For examples containing perylene bisimides, see: (a) Giaimo, J. M.; Gusev, A. V.; Wasielewski, M. R. *J. Am. Chem. Soc.* **2002**, 124, 8530–8531. (b) Ahrens, M. J.; Sinks, L. E.; Rybichinski, B.; Liu, W.; Jones, B. A.; Giaimo, J. M.; Gusev, A. V.; Goshe, A. J.; Tiede, D. M.; Wasielewski, M. R. *J. Am. Chem. Soc.* **2004**, 126, 8284–8294. (c) Langhals, H. *Helv. Chim. Acta* **2005**, 88, 1309–1343. (d) Van der Boom, T.; Hayes, R. T.; Zhao, Y.; Bushard, P. J.; Weiss, E. A.; Wasielewski, M. R. *J. Am. Chem. Soc.* **2002**, 124, 9582–9590.
- (15) For other bichromophoric systems, see: (a) Staab, H. A.; Riegler, N.; Diederich, F.; Krieger, C.; Schweitzer, D. *Chem. Ber.* **1984**, 117, 246–259. (b) Jockic, D.; Asfari, Z.; Weiss, J. *Org. Lett.* **2002**, 4, 2129–2132. (c) Yu, H.-H.; Pullen, A. E.; Büschel, M. G.; Swager, T. M. *Angew. Chem., Int. Ed.* **2004**, 43, 3700–3703. (d) Kadish, K. M.; Frémond, L.; Ou, Z.; Shao, J.; Shi, C.; Anson, F. C.; Burdett, F.; Gros, C. P.; Barbe, J.-M.; Guillard, R. *J. Am. Chem. Soc.* **2005**, 127, 5625–5631. (e) Chang, C. J.; Loh, Z.-H.; Shi, C.; Anson, F. C.; Nocera, D. G. *J. Am. Chem. Soc.* **2004**, 126, 10013–10020. (f) Pognon, G.; Boudon, C.; Schenk, K. J.; Bonin, M.; Bach, B.; Weiss, J. *J. Am. Chem. Soc.* **2006**, 128, 3488–3489. For a trichromophoric example, see: Yagi, S.; Yonekura, I.; Awakura, M.; Ezoe, M.; Takagishi, T. *Chem. Commun.* **2001**, 557–558.
- (16) (a) Neuteboom, E. E.; Meskers, S. C. J.; Meijer, E. W.; Janssen, R. A. J. *Macromol. Chem. Phys.* **2004**, 205, 217–222. (b) Wang, W.; Wan, W.; Zhou, H.-H.; Niu, S.; Li, A. D. Q. *J. Am. Chem. Soc.* **2003**, 125, 5248–5249. (c) Wang, W.; Li, L.-S.; Helms, G.; Zhou, H.-H.; Li, A. D. Q. *J. Am. Chem. Soc.* **2003**, 125, 1120–1121.
- (17) (a) *Calixarenes 2001*; Asfari, Z., Böhmer, V., Harrowfield, J., Eds.; Kluwer Academic Publishers: Dordrecht, 2001. (b) *Calixarenes Revisited*; Gutsche, C. D.; The Royal Society of Chemistry: Letchworth, 1998. (c) Böhmer, V.; *Angew. Chem., Int. Ed. Engl.* **1995**, 34, 713–745. (d) *Calixarenes in Action*; Mandolini, L.; Ungaro, R., Eds.; Imperial College Press: London, 2000.
- (18) Kenis, P. J. A.; Noordman, O. F. J.; Houbrechts, S.; van Hummel, G. J.; Harkema, S.; van Veggel, F. C. J. M.; Clays, K.; Engbersen, J. F. J.; Persoons, A.; van Hulst, N. F.; Reinhoudt, D. N. *J. Am. Chem. Soc.* **1998**, 120, 7875–7883.
- (19) See ref 17c and (a) Zhao, B.-T.; Blesa, M.-J.; Mercier, N.; Le Derf, F.; Sallé, M. *J. Org. Chem.* **2005**, 70, 6254–6257. (b) Yu, H.-h.; Xu, B.; Swager, T. M. *J. Am. Chem. Soc.* **2003**, 125, 1142–1143. (c) Scherlis, D. A.; Marzari, N. *J. Am. Chem. Soc.* **2005**, 127, 3207–3212.
- (20) (a) Schazmann, B.; Alhashimy, N.; Diamond, D. *J. Am. Chem. Soc.* **2006**, 128, 8607–8614. (b) Souchon, V.; Leray, I.; Valeur, B. *Chem. Commun.* **2006**, 4224–4226. (c) Kim, S. K.; Lee, S. H.; Lee, J. Y.; Bartsch, R. A.; Kim, J. S. *J. Am. Chem. Soc.* **2004**, 126, 16499–16506. (d) Leray, I.; Lefevre, J.-P.; Delouis, J.-F.; Delaire, J.; Valeur, B. *Chem. – Eur. J.* **2001**, 7, 4590–4598. (e) van der Veen, N.; Flink, S.; Deij, M. A.; Egberink, R. J. M.; van Veggel, F. C. J. M.; Reinhoudt, D. N. *J. Am. Chem. Soc.* **2000**, 122, 6112–6113. (f) Ji, H.-F.; Dabestani, R.; Brown, G. M.; Sachleben, R. A. *Chem. Commun.* **2000**, 833–834. (g) Jin, T.; *Chem. Commun.* **1999**, 2491–2492. (h) Unob, F.; Asfari, Z.; Vicens, J. *Tetrahedron Lett.* **1998**, 39, 2951–2954. (i) Jin, T.; Monde, K. *Chem. Commun.* **1998**, 1357–1358. (j) Grigg, R.; Holmes, J. M.; Jones, S. K.; Norbert, W. D. *J. Am. Chem. Soc., Chem. Commun.* **1994**, 185–187. (k) Aoki, I.; Sakaki, T.; Shinkai, S. *J. Chem. Soc., Chem. Comm.* **1992**, 730–732.
- (21) (a) Prins, L. J.; Reinhoudt, D. N.; Timmerman, P. *Angew. Chem., Int. Ed.* **2001**, 40, 2382–2426. (b) Rebek, J., Jr. *Chem. Commun.* **2000**, 637–643. (c) Böhmer, V.; Vysotsky, M. O. *Aust. J. Chem.* **2001**, 54, 671–677. (d) Conn, M. M.; Rebek, J., Jr. *Chem. Rev.* **1997**, 97, 1647–1668.
- (22) (a) Steyer, S.; Jeunesse, C.; Armspach, D.; Matt, D.; Harrowfield, J. In *Calixarenes 2001*; Asfari, Z., Böhmer, V., Harrowfield, J., Vicens, J., Eds.; Kluwer: Dordrecht, The Netherlands, 2001; pp 513–535. (b) Fochi, F.; Jacopozzi, P.; Wegelius, E.; Rissanen, K.; Cozzini, P.; Marastoni, E.; Fiscaro, E.; Manini, P.; Fokkens, R.; Dalcanale, E. *J. Am. Chem. Soc.* **2001**, 123, 7539–7552.
- (23) Seybold, G.; Wagenblast, G. *Dyes Pigm.* **1989**, 11, 303–317.
- (24) Zhao, Y.; Wasielewski, M. R. *Tetrahedron Lett.* **1999**, 40, 7047–7050.
- (25) Vysotsky, M. O.; Böhmer, V.; Würthner, F.; You, C.-C.; Rissanen, K. *Org. Lett.* **2002**, 4, 2901–2904.
- (26) Van der Boom, T.; Evmenenko, G.; Dutta, P.; Wasielewski, M. R. *Chem. Mater.* **2003**, 15, 4068–4074.
- (27) Hippius, C.; Schlosser, F.; Vysotsky, M. O.; Böhmer, V.; Würthner, F. *J. Am. Chem. Soc.* **2006**, 128, 3870–3871.
- (28) Hippius, C.; van Stokkum, I. H. M.; Zangrando, E.; Williams, R. M.; Würthner, F. *J. Phys. Chem. C* **2007**, 111, 13988–13996.
- (29) Hippius, C.; van Stokkum, I. H. M.; Zangrando, E.; Williams, R. M.; Würthner, F., manuscript in preparation.
- (30) (a) Al-Soufi, W.; Reija, B.; Novo, M.; Felekyan, S.; Kühnemuth, R.; Seidel, C. A. M. *J. Am. Chem. Soc.* **2005**, 127, 8775–8784. (b) Novo, M.; Felekyan, S.; Seidel, C. A. M.; Al-Soufi, W. *J. Phys. Chem. B* **2007**, 111, 3614–3624.
- (31) Würthner, F.; Ahmed, S.; Thalacker, C.; Debaerdemaeker, T. *Chem. Eur. J.* **2002**, 20, 4742–4750.
- (32) (a) Quante, H.; Müllen, K. *Angew. Chem., Int. Ed. Engl.* **1995**, 34, 1323–1325. (b) Nolde, F.; Pisula, W.; Müller, S.; Kohl, C.; Müllen, K. *Chem. Mat.* **2006**, 18, 3715–3725. (c) Jung, C.; Müller, B. K.; Lamb, D. C.; Nolde, F.; Müllen, K.; Bräuchle, C. *J. Am. Chem. Soc.* **2006**, 128, 5283–5291.
- (33) It is to note, that for all other compounds containing the green chromophore, no excitation spectra were recorded because of the insufficient wavelength correction for excitation spectra of our instrument above 800 nm, and exclusive emission of the green chromophore appears above 850 nm.
- (34) (a) Ford, W. E.; Kamat, P. V. *J. Phys. Chem.* **1987**, 91, 6373–6380. (b) Ford, W. E.; Hiratsuka, H.; Kamat, P. V. *J. Phys. Chem.* **1989**, 93, 6692–6696.
- (35) Please note for comparison, that in the femtosecond transient absorption spectra of arrays **or**, **ror**, and **oro** (see Figures S13 and S14 and the detailed discussion of the spectra of array **or** in Supporting Information) the negative band at 590 nm slightly shifts its maximum to 610 nm within the time frame of the experiment. The latter might be attributed to conformational changes of the red perylene bisimide dye, a behavior which is also known from single molecule spectroscopy for the red perylene bisimides bearing phenoxy substituents at the bay positions that were immobilized in a polymer matrix. It is known that local reorganizations in the vicinity of the molecule have an impact on the orientation of the phenoxy substituents of these red PBIs. For details, see: Hofkens, J.; Vosch, T.; Maus, M.; Köhn, F.; Cotlet, M.; Weil, T.; Herrmann, A.; Müllen, K.; De Schryver, F. C. *Chem. Phys. Lett.* **2001**, 333, 255–263. For a recent study for processes in solution, see: Osswald, P.; Leusser, D.; Stalke, D.; Würthner, F. *Angew. Chem., Int. Ed.* **2005**, 44, 250–253.
- (36) (a) Lukas, A. S.; Zhao, Y.; Miller, S. E.; Wasielewski, M. R. *J. Phys. Chem. B* **2002**, 106, 1299–1306. (b) Shibano, Y.; Umeyama, T.; Matano, Y.; Tkachenko, N. V.; Lemmetyinen, H.; Imahori, H. *Org. Lett.* **2006**, 8, 4425–4428.
- (37) See, for example: (a) Beechem, J. M.; Ameloot, M.; Brand, L. *Chem. Phys. Lett.* **1985**, 120, 466–472. (b) Ameloot, M.; Boens, N.; Andriessen, R.; Van Den Bergh, V.; De Schryver, F. C. *J. Phys. Chem.* **1991**, 95, 2041–2047. (c) Turkoni, S.; Schweitzer, G.; Holzwarth, A. R. *Photochem. Photobiol.* **1993**, 57, 113–119. (d) Roelofs, T.; Lee, C.; Holzwarth, A. R. *Biophys. J.* **1992**, 61, 1147–1163. (e) Ptacek, J.; Devgan, G.; Michaud, G.; Zhu, H.; Zhu, X.; Fasolo, J.; Guo, H.; Jona, G.; Breitkreutz, A.; Sopko, R.; McCartney, R. R.; Schmidt, M. C.; Rachidi, N.; Lee, S. J.; Mah, A. S.; Meng, L.; Stark, M. J. R.; Stern, D. F.; De Virgilio, C.; Tyers, M.; Andrews, B.; Gerstein, M.; Schweitzer, B.; Predki, P.F.; Snyder, M. *Nature* **2005**, 438, 679–684. (f) van Stokkum, I. H. M.; Larsen, D. S.; van Grondelle, R. *Biochim. Biophys. Acta* **2004**, 1657, 82–104. (g) van Stokkum, I. H. M.; Lozier, R. H. *J. Phys. Chem. B* **2002**, 106, 3477–3485. (h) Mullen, K. M.; van Stokkum, I. H. M. *J. Statistical Software* **2007**, 18. URL <http://www.jstatsoft.org/v18/i03/>. (i) Global and target analysis can be performed with, e.g., the R package TIMP, see <http://cran.r-project.org/doc/packages/TIMP.pdf>.
- (38) Note that in the SADS depicted in Figure 6 processes of 0.2 ps that have been assigned to fast solvent reorganization processes were omitted from the spectra for clarity. For details, see also Table 1 and: (a) Schweitzer, G.; Gronheid, R.; Jordens, S.; Lor, M.; De Belder, G.; Weil, T.; Reuther, E.; Müllen, K.; De Schryver, F. C. *J. Phys. Chem. A* **2003**, 107, 3199–3207. (b) De Belder, G.; Jordens, S.; Lor, M.; Schweitzer, G.; De, R.; Weil, T.; Herrmann, A.; Wiesler, U. K.; Müllen, K.; De Schryver, F. C. *J. Photochem. Photobiol. A* **2001**, 145, 61–70.
- (39) Note, that $k = k_{ET} + k_{CT}$ and $k_1 = 1/\tau$. Accordingly, with $1/\tau = 1/\tau_{ET} + 1/\tau_{CT}$, for example, for array **org** $\tau = 1.3$ ps, $\tau_{ET} = 1.4$ ps, and $\tau_{CT} = 12.0$ ps, respectively (see Table 2 and Table S1). For calculation details please also see the note 41 below.
- (40) Pullerits, T.; Heck, S.; Herek, J. L.; Sundström, V. *J. Phys. Chem. B* **1997**, 101, 10560–10567.
- (41) From the obtained rate constants, the efficiency of the energy transfer process E_{ET} as well as the efficiency of the competitive charge

transfer process E_{CT} can be calculated as follows with k_{ET} being the energy transfer rate (between neighboring PBI units) and k_{CT} the charge transfer rate (from the calix[4]arene moiety to the adjacent PBI chromophore): $E_{ET} = k_{ET}/k_{ET} + k_{CT} + k_{\pi} = 1/\tau_{ET}/1/\tau_{ET} + 1/\tau_{CT} + 1/\tau_D$ and $E_{CT} = k_{CT}/k_{ET} + k_{CT} + k_{\pi} = 1/\tau_{CT}/1/\tau_{ET} + 1/\tau_{CT} + 1/\tau_D$.

(42) An estimation of the Gibbs free energy of the photoinduced electron transfer (PET) process from the calix[4]arene to the red perylene bisimide moiety in CH_2Cl_2 reveals that this process is endergonic ($\Delta G_{CS} = +0.063$ eV, for details see Supporting Information, page S29). Therefore, it can be

concluded that the formation of a charge separated state consisting of the radical cation of the calix[4]arene moiety and the respective radical anion of the red perylene unit is energetically not favorable (see detail discussion in Supporting Information).

(43) Förster, T. *Ann. Phys.* **1948**, 55–75.

(44) *Molecular Fluorescence*; Valeur, B.; Wiley-VCH: Weinheim, 2002; pp 247–272.

(45) Rodríguez-Morgade, M. S.; Torres, T.; Atienza-Castellanos, C.; Guldi, D. M. *J. Am. Chem. Soc.* **2006**, *128*, 15145–15154.